



8th Manufacturing Engineering Society International Conference

Reverse engineering applied to biomodelling and pathological bone manufacturing using FDM technology

Laura Piles^a, Miguel J. Reig^{b*}, Vte. Jesús Seguí^b, Rafael Pla^c, Fernando Martínez^d, José Miguel Seguí^d

^a *Universitat Politècnica de Valencia – Pl. Ferrándiz y Carbonell, s/n, Alcoy 03801, Spain*

^b *Instituto de Tecnología de Materiales, Universitat Politècnica de Valencia – Pl. Ferrándiz y Carbonell, s/n, Alcoy 03801, Spain*

^c *Instituto de Diseño y Fabricación, Universitat Politècnica de Valencia – Pl. Ferrándiz y Carbonell, s/n, Alcoy 03801, Spain*

^d *Hospital Universitario de San Juan – Ctra. Nnal. 332, s/n, Sant Joan d'Alacant 03550, Spain*

Abstract

Reverse engineering and medical image-based modeling technologies allow manufacturing of 3D biomodels of anatomical structures of human body. These techniques are based on anatomical information from scanning data such as CT and MRI, whose scanners are used for scanning data acquisition of the external and internal geometry of anatomical structures. These 3D biomodels have many medical applications such surgical training, preoperative planning, surgical simulation, diagnosis and treatments. 3D virtual models of human body structures based on CT are increasingly being used in clinical practice. A data processing methodology is required to obtain an accurate 3D model suitable for manufacturing using AM, and specially the FDM technologies. This study shows a step-by-step methodology to process the CT information in bounded uncertainty conditions in order to obtain the STL models of the degenerated bone components, and to manufacture the 3D biomodels for surgery analysis with optimal design and details, and with an adequate accuracy to ensure proper results by surgeons analysis.

© 2019 The Authors. Published by Elsevier B.V.

This is an open access article under the CC BY-NC-ND license (<http://creativecommons.org/licenses/by-nc-nd/4.0/>)

Peer-review under responsibility of the scientific committee of the 8th Manufacturing Engineering Society International Conference

Keywords: FDM; Reverse Engineering; CT Data; Bones; Image Processing; Modeling Techniques; 3D Printing

* Corresponding author. Tel.: +34-966528422; fax: +34-966528422.

E-mail address: mjreig@mcm.upv.es

1. Background

The 3D models of bones and organs are more and more used in clinical practice for surgery simulations, preoperative planning, education, create reverse-engineered orthopedic implants, etc. [1] It has been increased in the last years due to the advanced medical engineering, which is getting better results with a high geometric accuracy.

The CT is the most used technique to scan the bones but CT imaging technologies and their acquisition parameters have an effect on the accuracy of medical data obtained [2]. In fact, the contrast provided by X-ray CT must be considered because it can make the segmentation easier for making the osseous structures more distinguished from surrounding soft tissue [3]. The result is a more detailed image of bones and soft tissues to be processed [4].

Nowadays there are several software that can process this information to create 3D model reconstructions; but a meticulous methodology should be applied in order to achieve good results with a high accuracy. The accuracy of these 3D models is essential to assure that surgeons analysis are reliable in order to improve the implants and prosthesis fitting to the patient morphology.

The disadvantage of this method is the extensive manual post-processing required. The image processing and segmentation of the CT data is the task that introduce the major inaccuracies in the process [5]. The AM and the FDM are suitable manufacturing technologies to obtain physical models of the initial bone geometries [6, 7], the dimensional accuracy of FDM processing depends on STL source and in-machine manufacturing conditions.

Nomenclature

RE	Reverse Engineering
CT	Computed Tomography
MRI	Magnetic Resonance Imaging
AM	Additive Manufacturing
FDM	Fused Deposition Modeling
STL	Standard Triangle Language
DICOM	Digital Imaging and Communication in Medicine
ABS	Acrylonitrile-Butadiene-Styrene

2. Methodology

2.1. Obtaining computed tomography data.

Four patients were selected for this study with the following bone pathologies: two of them with light osteoporosis, which need a full model analysis (scapula and humerus); one with severe osteoporosis, which needs a full model analysis too; and one with no osteoporosis but with humerus fracture, which only needs the scapula model analysis.

Patients CT images were obtained with a TOSHIBA Aquilion 16 scanner according to the established acquisition protocol at the Hospital Universitario of San Juan. The control volume for structures analysis were scanned using 120 kVp, with a slice thickness of 0.4 mm, and a FC06 convolution kernel for soft tissues and FC30 for bones. These scanner parameters are established to achieve a better visualization of the different body structures and determine the contrast between pixels according the Hounsfield scale (12 bits grey color scale with 4096 levels).

The CT image resolution is 512 x 512 pixels, so the pixel size can oscillate between 0.3 and 0.5mm due to the dimensions of acquisition volume, limited to reduce the patient X-ray exposure. This pixel size determines the initial accuracy limitation that can be expected in final 3D printed shape.

The CT data was saved in DICOM image format to be processed in further applications.

2.2. DICOM processing for bone segmentation.

The DICOM files were processed with 3D Slicer v4.8.1, which is an open source software for import and processing DICOM images to generate faceted models of specific human structures and tissues.

It is necessary to establish a region of interest (ROI) according to the dimensions of the humerus and scapula, such as to be able to identify almost the entire scapula and humerus in aim to define the more representative landmarks of their geometry. The ribs and the clavicle were rejected because they are not necessary to position the expected prosthesis after the surgeon analysis.

In order to get a better image resolution with a better approaching of STL model to bone profile, it is advisable to apply an interpolation method with B-Spline approaching to crop the ROI volume. The interpolation has to be adjusted for each patient in order to reduce the pixel size between the range [0.3, 0.4] mm, as well as it has to be activated the *Isotropic spacing* (perfect cubic voxel) option to ensure equal pixel size in three spatial axes (Fig. 1).

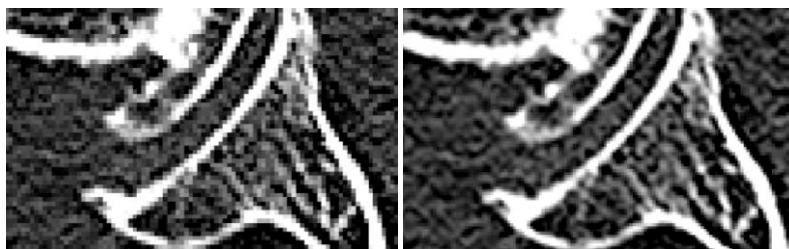


Fig. 1. Interpolated cropping with B-spline approaching for pixel size reduction from 0.45x0.45x0.4 mm (a) to 0.3x0.3x0.3 mm (b)

2.3. Image segmentation.

The different tissues of the human body have been determined according to the following values of the Hounsfield scale (Table 1).

Table 1. Hounsfield scale for some human body tissues.

Model	Minimum	Maximum
Cortical tissue	300	2200
Medullar tissue	-200	200
Muscle	10	40
Fat	-200	-50

To define the primary bone segmentation, the *Threshold* filter was applied with values above 300 Hounsfield units to determine the entire cortical tissue pixels in ROI. This procedure does not distinguish different bones in ROI volume, so all of them are considered as only one structure in this primary segmentation.

To distinguish these structures and define every single bone as an isolated structure, the *Islands* tool must be applied. Due to the pathological bones (osteoporosis or fractured bones) some structures cannot be isolated from the neighbor structures (Fig. 2). For this reason, manual processing of segments (*Erase* tool, slice by slice) is needed to put into different segment each structure (scapula, humerus, clavicle, osteofits, ...) and to achieve an accurate result.

Because of the patients pathology, the *Threshold* filter can obtain bones with several holes and empty zones that correspond to parts of the structure with a Hounsfield level outside the working range selected (Fig. 3). This problem is more pronounced in patients with severe osteoporosis and generates troubleshooting in STL reconstruction of external bone surface. From these incomplete structures, no useful STL models can be generated to 3D printing of solid bones.

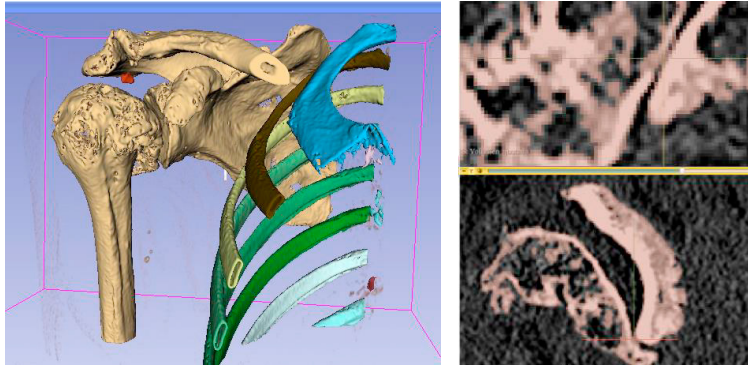


Fig. 2. Clavicle, humerus and scapula considered as one structure after applying the *Islands* filter (a) due to contact voxels (b).

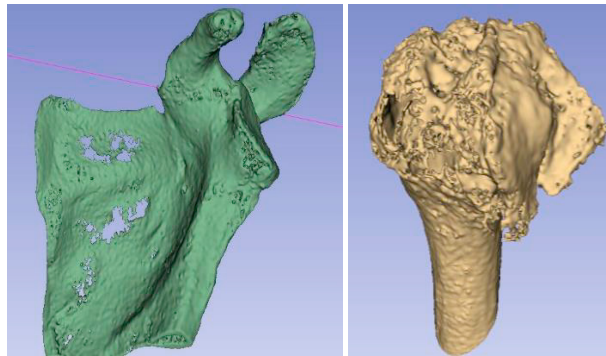


Fig. 3. Holes and discontinuous surfaces after applying the *Threshold* filter for scapula(a) and humerus (b).

So filling the holes of the scapula's body with manual filters is required to get a continuous surface of the bone. But for those areas that wrap medullar bone, the holes can be understood as tissue whose mechanical properties are worse than the ones of the cortical bone, especially in osteoporotic patients. In these cases, the *Grow from seeds* filter can be applied, so the medullar tissue can be extended to the exterior surface, filling the holes and generating a solid suitable to be printed (Fig. 4).

So, the medullar tissue in all the patients was defined using the *Grow from seeds* filter and considering values in Hounsfield units between -150 and 299. The application of this filter on the bone geometry of patients with osteoporosis has to be intensified in the most affected areas to achieve a more accurate result.

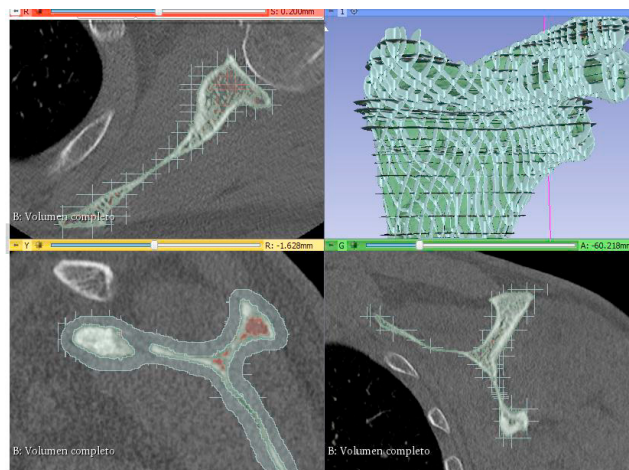


Fig. 4. *Grow from seeds* filter applied to an osteoporotic scapula (green segment = cortical tissue, grey segment = external area, brown segment = medullar tissue).

For guarantee that the use of the *Grow from seeds* filter has a minimum error, it is required the application of the *Masking* filter with the following parameters:

- *Editable area*: Outside all visible segments (what prevents overwrite seeds already created).
- *Editable intensity range*: disabled (preferable) or activate with the range outside the initial segment to avoid its modification.
- *Overwrite other segment*: None (prevents the already created segments from being overwritten).

Once the cortical tissue segment has no holes and the medullar tissue segment has been created after applying the *Grow from seeds* filter (Fig. 5), they can be combined as a unique and solid structure to generate the STL model. Using the *Logical Operators* tool, it is possible to copy the information from a segment (*Copy*) and add the one from others (*Add*) to rebuild a segment with cortical and medullar bone.



Fig. 5. Cortical (yellow) and medullar (red) tissue of scapula isolated in different segments.

A defect that appears in the segments reconstruction is noisy voxels produced by unexpected Hounsfield values. These noisy voxels need to be removed from segments in order to avoid small details in FDM processing. These defects are especially critical in osteoporosis pathologies. With the *Closing* filter the voids inside the model can be removed for getting a solid STL model to print; while the *Opening* filter can avoid the surface protrusions producing soft and regular 3D printing paths (Fig. 6). These filters are applied over the neighborhood of each voxel and are voxel size dependents. For example, for a neighborhood of 3x3x3 pixels, the size of noise/protrusions voxels avoided can vary from 0.9 mm to 1.5 mm. This detail justifies the ROI volume interpolation of section 2.2 in order to reduce the voxel size and, therefore, extend the filter application to small details. In this study, the combination of *Grow* filter (3x3x3), *Opening* filter (3x3x3), *Shrink* filter (3x3x3) and *Closing* filter (3x3x3) have produced optimal results on final bone shape.

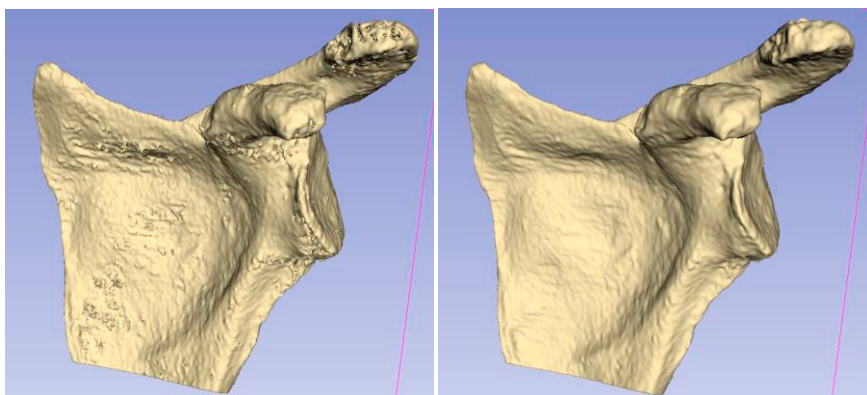


Fig. 6. Results of *Smoothing* filters for noisy voxels deletion (b) from initial model (a).

2.4. Facet model generation and 3D printing.

3D Slicer software allows generate faceted models from segmentation that can be exported to 3D printing file formats: STL, PLY, OBJ and VTK. Usually only the OBJ and STL file formats are suitable for 3D printing because they are recognized by available and widely used printing software (*Ultimaker Cura, Slic3r, ...*).

The software model fitting to STL from segmentation uses B-spline approaching (Fig. 7), so the model accuracy can be expected according the Eq. 1.

$$\Delta I_{STL} = \sqrt{\left(\frac{\Delta x_{slice}}{2}\right)^2 + \left(\frac{\Delta y_{slice}}{2}\right)^2 + \left(\frac{\Delta z_{slice}}{2}\right)^2} \quad (1)$$

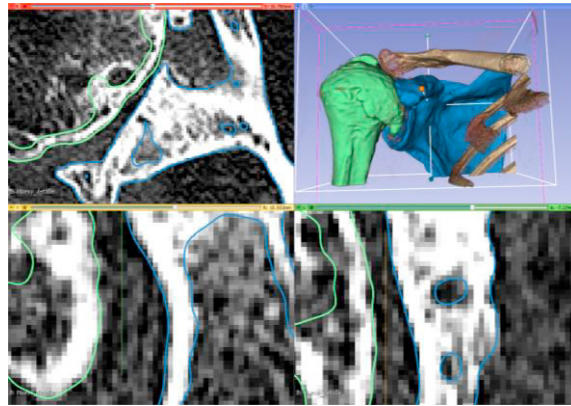


Fig. 7. STL model approximation in glenoid area (green = cortical humerus model, blue = cortical scapula model).

The STL models of bones are ready to use by 3D printing software; but some printing considerations must be regarded to obtain better results:

- The nozzle diameter should be 0.4 mm or less in order to minimize the path rounding errors and assure that they do not exceed from 0.2 mm.
- Working with low print speed (between 10 and 25 mm/s) and small layer height (from 0.1 to 0.2 mm) is required.
- It is preferable to use ABS material because its shrinkage is bounded and low [0.4 to 0.7%]. For this material is advisable to use the lowest printing temperature to avoid an excessive thermal rise that increase the shrinkage.
- The wall thickness should be greater than or equal to 0.8 mm to guarantee the model's strength.
- The infill density must be established between 10 and 20% due to the model's strength and material's low consumption.
- In order to easily remove the support and raft material from model, the Z distance from support and the raft air gap have been established in 0.1 mm. These parameters allow an accurate removing of these waste materials.

2.5. Results.

In accordance with the recommendations indicated in this study, the cases studied have been processed with relative simplicity (Figs. 8 to 10). FDM models processing have been carried out with Ultimaker Cura 3.6.0 from Ultimaker B.V., and FDM manufacturing has been carried out with a XYZPrinting Da Vinci 1.0 Pro printer and with Sakata ABS-E material with abovementioned processing parameters.

The Traumatology team of the Hospital de San Juan has evaluated these results; and the diagnosis of the pathology of the patients has been improved and the surgical intervention has been planned in advance quickly and efficiently.

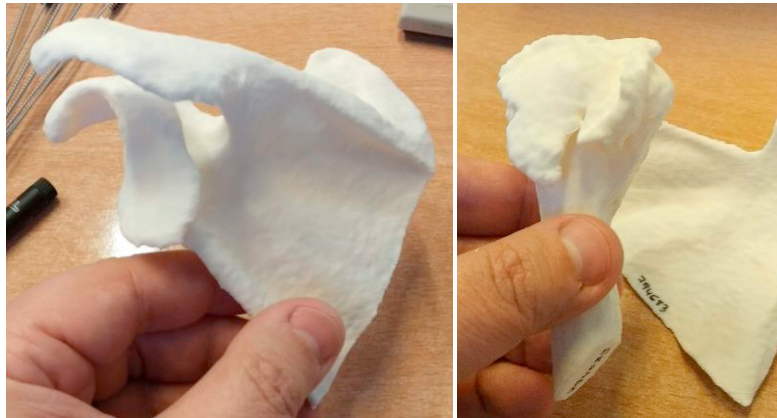


Fig. 8. 3D Models of severe osteoporotic deformation of scapula glenoid (a) and humerus head (b).



Fig. 9. 3D Model of scapula and glenoid area of patient with humerus head fracture.

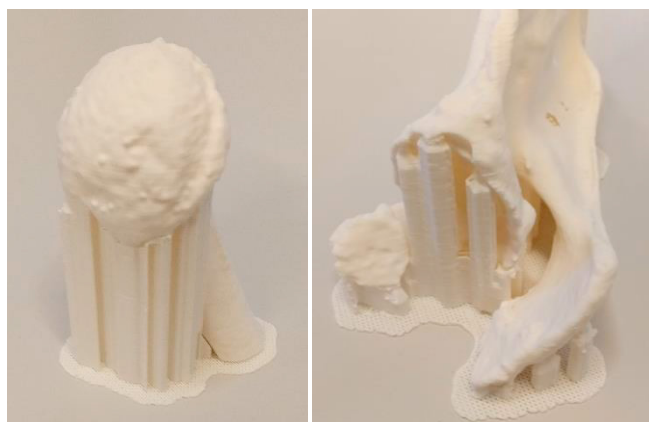


Fig. 10. 3D printed models (model+support+raft) of osteoporotic deformation of humerus head (a) and glenoid area (b).

Printed models have been checked with a tracking laser scanner in order to evaluate their accuracy from STL model, obtaining the deviation shown in Fig. 11.

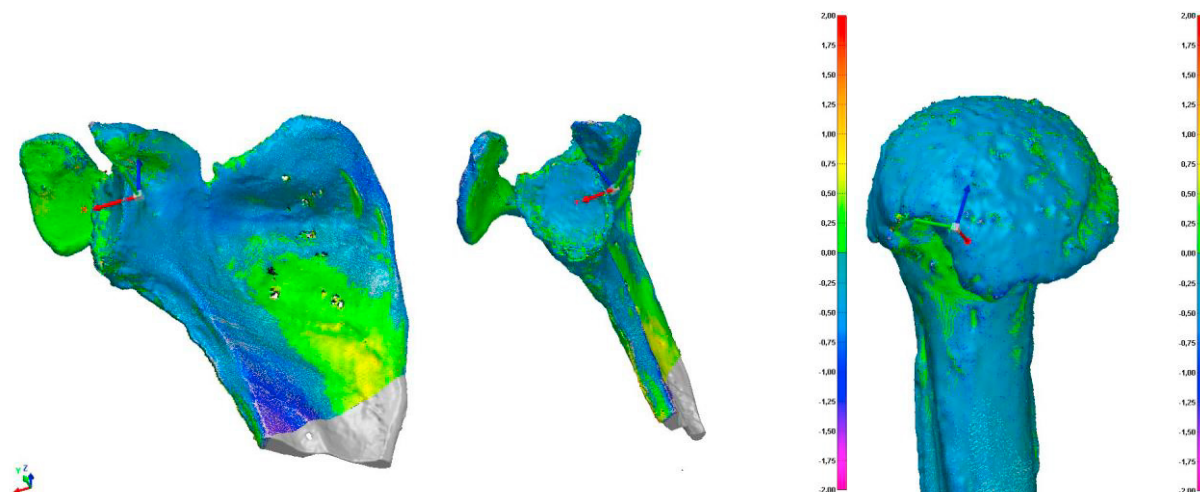


Fig. 11. Printed models vs. STL models checking (distance in mm) of scapula (a) and humerus (b).

3. Conclusions

This paper summarizes a recent integrated research between traumatology team of Hospital de San Juan and manufacturing engineers from Universitat Politècnica de València to establish and apply a specific methodology to analyze the geometrical CT information and to manufacture 3D printed models of bone structures for pre-surgical analysis. The application of this methodology has improved the pathology diagnosis, has reduced the time of surgical intervention, and has improved the placement of prostheses. In further studies, these results have been used to develop the geometric design of guiding tools to improve the final prosthesis positioning.

Acknowledgements

The authors wish to acknowledge the support of Ms. Jerica Risent and Mr. Joan Ortiz of Ford Motor Company for his assistance in the scanning of printed models. This work was supported by the Polisabio Funding (UPV-Fisabio 2017).

References

- [1] J. Wolff, A. Mäkitie, M. Salmi, J. Tuomi, K.S. Paloheimo, Accuracy of medical models made by additive manufacturing (rapid manufacturing), *Journal of Cranio-Maxillofacial Surgery*, 41-7 (2013) 603-609
- [2] M. Van Eijnatten, F. H. Berger, P. De Graaf, J. Koivisto, T. Forouzanfar, J. Wolff, Influence of CT parameters on STL model accuracy, *Rapid Prototyping Journal*, 23-4 (2017) 678-685
- [3] E. A. Lalone, R. T. Willing, H. L. Shannon, G. J. W. King, and J. A. Johnson, Accuracy assessment of 3D bone reconstructions using CT: An intro comparison, *Medical Engineering & Physics*, 37-8 (2015) 729-738
- [4] K. E. Stull, M. L. Tise, Z. Ali, and D. R. Fowler, Accuracy and reliability of measurements obtained from computed tomography 3D volume rendered images, *Forensic Science International*, 238 (2014) 133-140
- [5] M. van Eijnatten, R. van Dijk, J. Dobbe, G. Streekstra, J. Koivisto, J. Wolff, CT image segmentation methods for bone used in medical additive manufacturing, *Medical Engineering & Physics*, 51 (2018) 6-16
- [6] M. Javaid, A. Haleem, Additive manufacturing applications in medical cases: A literature based review, *Alexandria Journal of Medicine*, 54 (2018) 411-422
- [7] D.V.C. Stoffelen, K. Eraly, P. Debeer, The use of 3D printing technology in reconstruction of a severe glenoid defect: a case report with 2.5 years of follow-up, *Journal of Shoulder Elbow Surgery*, 24 (2015) e218-e222